J|A|C|S
ARTICLES
Published on Web 02/23/2008

The Role of Conformation in Ion Permeation in a K^+ Channel

Carmen Domene,*[,†,‡] Satyavani Vemparala,[‡,§] Simone Furini,[†] Kim Sharp,[||] and Michael L. Klein[‡]

Physical and Theoretical Chemistry Laboratory, Department of Chemistry, University of Oxford, Oxford OX1 3QZ, U.K., Department of Chemistry and Center for Molecular Modeling, University of Pennsylvania, 231 South 34th Street, Philadelphia, Pennsylvania 19104-6323, The Institute of Mathematical Sciences, C.I.T Campus, Taramani, Chennai 600 113, India, and Department of Biochemistry and Molecular Biophysics, University of Pennsylvania, 37th and Hamilton Walk, Philadelphia, Pennsylvania 19104-6059

Received July 11, 2007; E-mail: carmen.domene@chem.ox.ac.uk

Abstract: The chemical-physical basis for K^+ permeation and selectivity in K^+ channels has been the focus of attention of many theoretical and computational studies since the first crystal structure was obtained by the Mackinnon lab in 1998. Most of the previous studies reported focused on atomic descriptions of permeation events in the selectivity filter of K^+ channels in their closed conformation. In this Article, a comparative analysis of permeation events in the KirBac1.1 K^+ channel in a closed- and an open-state model is presented. The availability of models of the same channel in two different conformations has made this comparative analysis possible. All-atom molecular dynamics simulations of both models in a membrane environment have been carried out. As previously suggested by many studies of this and other K^+ channels, when the channel is closed the ion conduction involves transitions between two main sites of the selectivity filter, with two K^+ ions each coordinated by eight carbonyl oxygens of the protein and separated by a water molecule. In contrast, in our open-state model, three to four K^+ ions move in a concerted motion during the permeation process. The selectivity filter, though maintaining a certain degree of flexibility to cope with these cooperative events, appears to be more "symmetrical" and robust in the simulations of the open-state channel when it is occupied by an average of three ions. Therefore, it appears as if the occupation of the pore depends upon the global conformation of the channel. Due to the complexity of these systems, only single conduction events have been described by means of molecular dynamics trajectories. To complement these results and describe the energetics of ion permeation and ionic fluxes, continuum approaches (Poisson−Boltzmann and Poisson−Nernst−Planck theory) have been also employed.

Introduction

The KirBac1.1 channel belongs to the inward rectifier family of K^+ selective ion channels. Inward rectifier channels have two main physiological roles: they are involved in K^+ transport across membranes and they regulate cell excitability by stabilizing the membrane potential close to the K^+ equilibrium potential. In particular, Kir1 channels are important for electrolyte flow across kidney epithelial cells.[1] Inward rectification refers to the fact that under physiological conditions, Kir channels exhibit higher conductance for K^+ flowing into the cell.[2] The inward rectification in Kir channels is caused by blockers such as Mg^{2+} ions or polyamines[3] that hindered the movement of K^+ ions in the outward direction where the electrochemical gradient favors the outward flow of K^+. The three-dimensional structure of KirBac1.1 was first reported in the closed state at 3.65 Å resolution.[4] KirBac1.1 is a tetramer with a core pore-forming transmembrane (TM) domain. This TM domain is composed of a M1-P-F-M2 motif, where M1 and M2 are helices, P is a short helix, and F is the extended filter region. The selectivity filter adopts an extended strand conformation where the carbonyl oxygens of the backbone point toward the lumen orchestrating the movements of ions in and out of the channel. The selectivity filter is identical to the KcsA K^+ channel, suggesting that the mechanism for K^+ selection is likely to be the same. Below the selectivity filter, the channel opens into a wide chamber connected to the intracellular space by a hydrophobic pore. The intracellular (IC) domain of Kirbac1.1 consists mostly of β-sheet, with a fold related to the IC domain of the KirBac3.1 channel. The IC domain contains mainly polar and charged residues and constitutes two-thirds of the amino acid sequence of the channel. Negatively charged

† University of Oxford.
‡ Department of Chemistry and Center for Molecular Modeling, University of Pennsylvania.
§ The Institute of Mathematical Sciences, C.I.T. Campus.
|| Department of Biochemistry and Molecular Biophysics, University of Pennsylvania.

(1) Hebert, S. C.; Desir, G.; Giebisch, G.; Wang, W. H. *Phys. Rev.* **2005**, *85*, 319−371.
(2) Lu, Z. *Annu. Rev. Phys.* **2004**, *66*, 103−129.
(3) Ruppersberg, J. P. *Pfluegers Arch.* **2000**, *441*, 1−11.
(4) Kuo, A.; Gulbis, J. M.; Antcliff, J. F.; Rahman, T.; Lowe, E. D.; Jochen, Z.; Cuthbertson, J.; Ashcroft, F. M.; Ezaki, T.; Doyle, D. A. *Science* **2003**, *300*, 1922−1926.

residues are strategically located along the ion conduction pathway which, as well as acting as a simple screen to repel anions, form binding sites that regulate the flow of ions. In the KirBac1.1 structure, there are two double rings of negatively charged glutamate residues located in the vestibule region on the intracellular side of the membrane. These rings of negatively charged amino acids are thought to be important in ion binding and in ion conduction.

In the closed channel two constrictions, at the inner helix bundle and at the apex of the cytoplasm pore, block the ion conduction pathway, serving as intracellular gates. The helix bundle consists simply of four hydrophobic phenylalanine residues (Phe146), located at the interface between the membrane and the cytoplasm. In order for the KirBac1.1 channel to move into the open state, these hydrophobic Phe residues must be displaced from their centrally located position in the closed state. The diameter of the intracellular mouth in closed form is about 4 Å, which prevents any ion flux through the channel. How K^+ channels can be highly selective, what the chemical basis is by which the channel distinguishes between K^+ and other alkali ions, and how channels reshape the energetic landscape to facilitate ion passage remain fundamental questions, with important implications for understanding ion channel function and the effects of drugs and blockers.

The physicochemical basis of the transport of K^+ ions through the selectivity filter of these K^+ channels has been the focus of many studies using the closed conformation of the current available crystal structures.[5−9] Fewer studies have been reported aiming at describing conformational changes which might take place during the gating process. Compoint et al.[10] applied a targeted molecular dynamics (MD) procedure to simulate the gating mechanism of the KcsA channel subject to an opening constraint. The constraint was applied starting from the crystallized closed structure and moving toward a partially known open form, derived from electron paramagnetic resonance experiments. During the relaxation of the protein, diffusion of K^+ ions toward the extracellular side is observed on a small time scale. It remains to be determined whether the motions of the K^+ ions could be the origin of large displacements of the M_2 helices and vice versa.

Chung and Allen[11] and Biggin and Sansom[12] have independently performed steered MD to obtain models of KcsA open states. Chung and Allen pulled the TM helices outward and artificially stabilized the aperture at the desired configuration by placing a repulsive cylinder inside the open pore, while Biggin and Sansom generated open states by placing a van der Waals balloon at the intracellular mouth of the channel and gradually inflating it as a function of time. When relaxed, these different metastable structures led to a wider pore radius at the intracellular region and indicated that there should be a preferred pathway to the open state.

In this paper, an open model of KirBac1.1 based on two-dimensional electron microscopic data is adopted. This KirBac1.1 open-state model was obtained using the channel structure in its X-ray closed conformation (1P7B).[13] The initial open-state model was refined by using projection maps obtained from electron microscopy experiments on two-dimensional crystals of the inwardly rectifying K^+ channel KirBac3.1 from *Magentospirillum magnetotacticum* captured in its open state. It was hypothesized that the transmembrane helices moved away from the central ion conduction pathway by bending approximately halfway along their length. This arrangement resulted in a mouth of 12 Å diameter which connected the high-dielectric bulk solution to the anisotropic dielectric environment of the channel pore. To test the validity of the open-state model, MD simulations in octane, a lipid bilayer mimetic, were performed,[14] and it was found that the open-state model was stable during several simulations of tens of nanoseconds, with a total simulation time of over 138 ns.

In this study, a comparative analysis of permeation events in the KirBac1.1 channel in the closed- and open-state models is presented. Ion−protein interactions and the translocation of K^+ ions along the selectivity filter will be described on the basis of MD simulations. MD simulations with explicit solvent, membrane, protein, and ions provide a realistic representation of these complex systems; however, the time scale of permeation events is notably longer than what can be achieved. Therefore, in order to describe permeation characteristics, the Poisson−Boltzmann (PB) and Poisson−Nernst−Planck (PNP) electrodiffusion theories have been employed. In these approaches, the protein is treated as a rigid structure, so atomic thermal fluctuations are neglected, while hydration effects are absent due to the representation of the solvent as a continuum dielectric medium. These approaches are computationally less expensive than MD simulations, and despite their limitations, contributions from all of them will certainly assist in the understanding of ion permeation.

Materials and Methods

Model Definitions. First, the DOPC lipid bilayer was built by replicating a small equilibrated patch.[15] The 340 DOPC bilayer was then equilibrated for 5 ns before the insertion of either the closed or open-state models of KirBac1.1. Both the closed- and open-state models were inserted into the bilayer by aligning the protein's axis of symmetry with the bilayer normal. The C-terminal carboxylate was protonated, and the N-terminal amine was unprotonated to form neutral termini. The program *Whatif* (www.cmbi.kun.l/whatif) was used to perform pK_a calculations to aid in assigning side-chain ionization states. On the basis of these calculations, the side chains of Asp115 were protonated. The rest of the residues remained in their default ionization states.

Lipids located within 1 Å of the protein were removed, and the system was then solvated using the *Solvate* plug-in of VMD,[16] ensuring adequate hydration of the protein above and below the lipid membrane. The total charge of the system was −8 in both the open and the closed conformations; ions were placed randomly corresponding to a salt concentration of ∼150 mM using the *Autoionize* plug-in of VMD to ensure that the system was neutral. Water molecules were added in the cavity of both open and closed-state models of KirBac1.1. The distance between images of the protein in both cases was >25 Å. Table

(5) Ban, F. Q.; Kusalik, P.; Weaver, D. F. *J. Am. Chem. Soc.* **2004**, *126*, 4711−4716.
(6) Åqvist, J.; Warshel, A. *Biophys. J.* **1989**, *56*, 171−182.
(7) Guidoni, L.; Carloni, P. *Biochim. Biophys. Acta* **2002**, *1563*, 1−6.
(8) Berneche, S.; Roux, B. *Nature* **2001**, *414*, 73−77.
(9) Domene, C.; Sansom, M. S. P. *Biophys. J.* **2003**, *85*, 2787−2800.
(10) Compoint, M.; Picaud, F.; Ramseyer, C.; Girardet, C. *J. Chem. Phys.* **2005**, *122*, 134707.
(11) Allen, T. W.; Chung, S. H. *Biochim. Biophys. Acta* **2001**, *83−91*, 15515.
(12) Biggin, P. C.; Sansom, M. S. P. *Biophys. J.* **2002**, *82*, 2530.
(13) Kuo, A.; Domene, C.; Johnson, L.; Doyle, D.; Venien-Bryan, C. *Structure* **2005**, *13*, 1463−1472.
(14) Domene, C.; Doyle, D.; Venien-Bryan, C. *Biophys. J.* **2005**, *89*, L1−L3.
(15) http://persweb.wabash.edu/facstaff/fellers/.
(16) Humphrey, W.; Dalke, A.; Schulten, K. *J. Mol. Graphics* **1996**, *14*, 33-&.

Table 1. System Composition of the Open and Closed Systems

	closed	open
lipids	266	253
water (bulk)	25 836	25 559
water (filter)	3	3
water (cavity)	28	39
K^+ (bulk)	77	79
K^+ (filter)	3	3
Cl^- (bulk)	72	74
total number of atoms	131 370	129 035

1 shows the number of atoms, lipids, water molecules, and ions in each of the systems.

Only one configuration of ions in the selectivity filter was used in both the closed- and open-state systems. The definition of each of the sites in KirBac is as follows: sites S1 to S4 form the selectivity region per se; an additional site, S0, equivalent to that in KcsA, is also considered at the external mouth. Each of these sites is defined as the center of two rings of four oxygen atoms. Site S1 is formed by the carbonyl oxygens of residues Tyr113 and Gly114 of each of the four monomers, S2 is formed by the carbonyl oxygens of Gly112 and Tyr113, and S3 is formed by the carbonyl oxygens of residues Val111 and Gly112. Site S4, next to the central cavity, is formed by one ring of carbonyl oxygen and another ring of hydroxyl oxygens from the side chains of the same residue Thr110. Finally, S0 is defined by the carbonyls of Gly114, which provide four oxygen atoms, with the remaining four oxygens being donated by water molecules at the extracellular mouth. Ions were placed in S0, S1, and S3, and a water molecule was placed in S2 and S4. The limits of the water-filled cavity were defined with the upper side located at Ala109 and the lower side ending at Ala150. That corresponds to dimensions of about 27 Å in length and 15 Å width at its maximum.

Molecular Dynamics (MD). MD simulations were performed using the NAMD package.[17] The CHARMM 22[18] and CHARMM 27[19] forcefields were used for the proteins and lipids, respectively, using a cutoff of 12 Å for nonbonded interactions. To establish the sensitivity of the results to changes in the ion parameters, two different parameter sets were used. In one set, all the ions (bulk and filter ions) were described by the default CHARMM parameters for ions. In the second set, the parameters for ions initially situated in the selectivity filter were chosen as described in ref 20. No apparent differences in the behavior of the ions were observed, though differences might emerge if detailed energetic profiles were calculated.

A conjugate−gradient-based minimization was first performed to remove any bad contacts. This was followed by a 300 ps run in which the protein, ions, and water in the filter were fixed to allow relaxation of the lipids and water around the protein. The particle mesh Ewald (PME) method was used to treat the electrostatics interaction. Constant pressure simulations were performed using the Nose−Hoover Langevin piston method for 3 ns, followed by 17 ns of constant volume simulations. Due to the large system size, the volume did not noticeably vary after the 2 ns equilibration run and the system size justifies the usage of a constant volume protocol. A time step of 1 fs was used for the computation of bonded potential terms, and a multiple time step method was employed for nonbonded interactions, wherein PME electrostatics calculations were computed every two steps.

Continuum Electrical Calculations. Poisson−Boltzmann (PB). In PB calculations, the last frame of each simulation was used for the system setup. All the channel atoms and the lipid bilayer were represented implicitly. Just one permeating ion was treated explicitly by placing it at a series of positions within the pore in both the closed- and open-state models; the ion trajectory was assumed to be straight along the *z* axis. The channel inserted in the lipid bilayer was centered at the origin with the pore aligned along the *z* axis of the Cartesian coordinate system. Electrostatic energies were calculated using the finite difference PB methodology.[21−23] The grid dimensions were 193 × 193 × 193, with a scale of ∼1 grid/Å. Solutions were obtained for the nonlinear Poisson equation, with Coulombic boundary conditions,[21] using the multigrid method of iteration.[24] The radii and charge values used were taken from Dieckmann et al.,[25] while the solvent and protein relative dielectric constants were 80 and 2, respectively.

Poisson−Nernst−Planck (PNP). PNP theory describes the steady-state fluxes of *N* ion species by the Poisson and Nernst−Planck equations

$$\nabla\cdot(\epsilon\nabla\phi) = -\rho - \sum_{i=1}^{N} z_i e C_i \tag{1}$$

$$\nabla\cdot J_i = 0 \qquad i = 1,...,N$$

$$J_i = -D_i\left(\nabla C_i + z_i \frac{e}{kT} C_i \nabla\phi\right) \tag{2}$$

where ϕ is the electric potential; C_i, D_i, J_i, and z_i are the concentration, the diffusion coefficient, the flux, and the valence of the *i*th ion species; ρ is the density of fixed electric charge and ϵ is the dielectric constant; and *e*, *k*, and *T* are the elementary charge, the Boltzmann constant, and the temperature. In the Poisson equation (eq 1) ρ is, in this case, equal to the charge due to the protein atoms, and, in contrast to the ionic charge, is fixed in space. Only the protein charge distribution was modeled, and the lipid bilayer was assumed to be electrically neutral. Two monovalent ion species were included in the mathematical model to simulate K^+ and Cl^- ions, respectively.

Channel models, atomic radii, partial atomic charges, and dielectric constants were defined as in the PB calculations. Outside the channel, the diffusion coefficients were set to the experimental values for diffusion in free solution ($D_{K^+} = 1.96 \times 10^{-9}$ m^2/s and $D_{Cl^-} = 2.03 \times 10^{-9}$ m^2/s). Inside the channel, these values were reduced to 10% of their original value as in ref 26. PNP equations were solved by an iterative algorithm, with a tolerance of 10^{-10} mV for the Poisson equations and 10^{-10} mM for the Nernst−Planck equation. Boundary conditions on electric potential were defined to simulate a membrane potential of −100 mV, while ion concentrations were set to 100 mM, both at the extracellular and intracellular boundaries. PNP calculations were performed on several snapshots extracted from the MD trajectory of the open channel model at 5, 10, 15, and 20 ns. Analyses confirmed that the main conclusions were not affected by the choice of snapshot.

Results and Discussion

Structure Stability. To assess the degree of conformational drift of the closed- and open-state models, the Cα root-mean-square deviation (rmsd) from the initial structure as a function of time was analyzed in each simulation. Figure 1.A shows the rmsd values for the protein and for various structural elements of the channels: M1 and M2 helices, selectivity filter (F), intracellular domain (IC), and slide helices (SH). Values are in

(17) Kale, L.; Skeel, R.; Bhandarkar, M.; Brunner, R.; Gursoy, A.; Krawetz, N.; Philips, J.; Shinozaki, A.; Varadarajan, K.; Schuten, K. *J. Comput. Phys.* **1999**, *151*, 283−312.
(18) MacKerell, A. D. et al. *J. Phys. Chem. B* **1998**, *102*, 3586−3616.
(19) Feller, S. E.; Yin, D.; Pastor, S. E.; MacKerell, A. D. *Biophys. J.* **1997**, *73*, 2269−2279.
(20) Roux, B.; Berneche, S. *Biophys. J.* **2002**, *82*, 1681−1684.
(21) Gilson, M. K.; Sharp, K. A.; Honig, B. H. *J. Comput. Chem.* **1988**, *9*, 327−335.
(22) Sharp, K. A.; Honig, B. *Annu. Rev. Biophys. Biophys. Chem.* **1990**, *19*, 301−332.
(23) Nicholls, A.; Sharp, K. A.; Honig, B. *Proteins: Struct., Funct., Genet.* **1991**, *11*, 281.
(24) Sharp, K. A.; Friedman, R. A.; Misra, V.; Hecht, J.; Honig, B. *Biopolymers* **1995**, *36*, 245−262.
(25) Dieckmann, G. R.; Lear, J. D.; Zhong, Q.; Klein, M. L.; DeGrado, W. F.; Sharp, K. A. *Biophys. J.* **1999**, *76*, 618−630.
(26) Furini, S.; Zerbetto, F.; Cavalcanti, S. *Biophys. J.* **2006**, *91*, 3162−9.

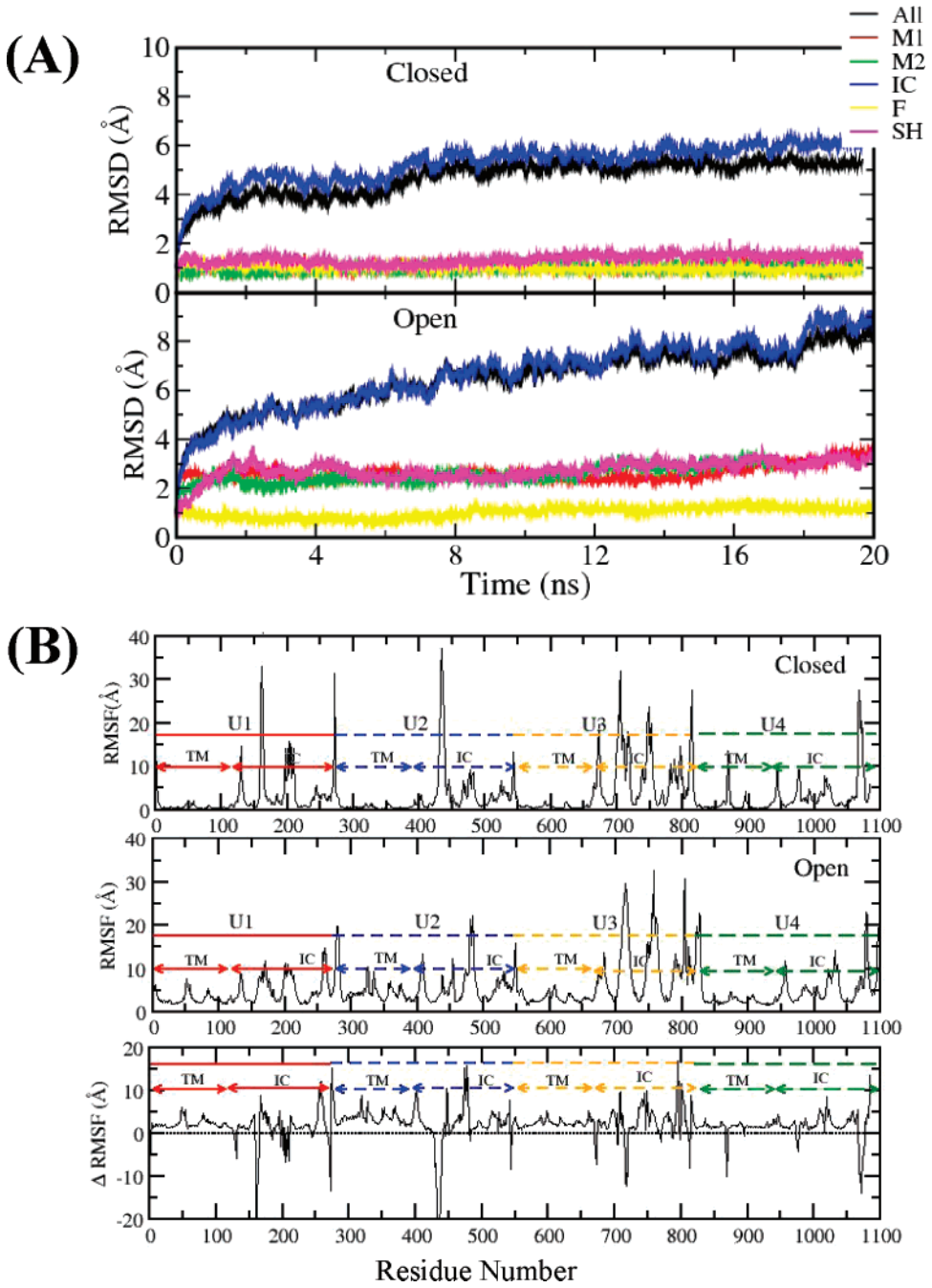

Figure 1. (A) Cα atom rmsd from the crystal structure (top panel) and the open-state model (bottom panel) vs simulation time. Values are as noted: for the protein in black; the intracellular domain (IC) in blue; the M2 and M1 helices in green and red, respectively; slide helices (SH) in magenta; and the selectivity filter (F) in yellow. (B) Cα root-mean-square fluctuations (rmsf) as a function of residue number for the closed- and open-state models. U1 to U4 corresponds to each of the four monomers; TM is the transmembrane domain and IC is the intracellular domain. In the bottom panel, the Δrmsf (closed-open) is also reported.

general higher in the case of the open-state system, reflecting the nature of the model. However, in both cases, the major rise seems to be in the initial 3 ns period. In the closed model, rmsd values for the M1, M2, and slide helices are ∼0.1 nm for M1/M2 and 0.15 nm for the slide helices. In the open-state model, these values increase to ∼0.3 nm for M1/M2 and slide helices. In both cases, the rmsd for the filter region is low (∼0.1 nm) and remains constant during the simulation. It is noteworthy that the IC domain and slide helices have quite high rmsd values. This can be attributed to the fact that three small segments were built into the model in the IC domain (they were missing in the initial model) and that there is a great deal of flexibility of the loop on the C-terminal domain that interacts with the N-terminus. The high rmsd of the slide helices can be accounted for by the lack of interactions with the lipid headgroups.

The fluctuations in the structure as a function of the residue number were evaluated in terms of Cα root-mean-square fluctuations (rmsf). To compute the rmsf values, all the frames in the last 10 ns of simulation were fitted to a common reference point to remove the effects of any translational and rotational motions in the molecule (Figure 1b). The mean fluctuation of the core TM domain (M1, P, and M2) in the closed- and open-state models is less than 1 and ∼2.5 Å, respectively. In general, rmsf values are higher in the open-state model than in the closed-

state model; see Figure 1b bottom panel for a plot of the Δrmsf (closed-open). In these simulations the slide helices and IC domains exhibit greater fluctuations than the other constituents in both models. The higher values of rmsf in the intracellular region correspond to loops lining the central pore. The lack of interaction between the N and C termini in our models, particularly in the open-state model, might be the reason for the high rmsf. The nature of the lipid−protein interactions involving the slide helices (first 10 residues of each monomer) may play a role in controlling the gating. The lack of some of these interactions might be another reason for the high drift values. In both simulations, the rmsf is quite low in the filter region. In Figure 1b, residues corresponding to the selectivity filter are (72−76, 343−347, 614−618, 885−889) and (75−79, 349−353, 623−627, 897−901) in the closed- and open-state models, respectively, and U represents one of the four monomers with index 1 to 4.

Structural Waters and Water in the Cavity. The high-resolution structure of KcsA (2.0 Å resolution) revealed four oxygen atoms from four water molecules sitting behind the selectivity filter. These water molecules hydrogen bond to the amide nitrogen of Glu71 and participate in an H-bond network between residues Glu71 and Asp80.[27] It was reported that the movement of these crystallographic waters does not seem to be correlated to the concerted translocations of the ions and water in the selectivity filter in MD simulations of the KcsA closed model in lipid bilayers.[9] Water molecules were not present at the back of the selectivity filter of KirBac1.1 in the crystal structure, and they were not included in the a priori models. However, four water molecules traveled from bulk solution to reach these sites and during most of the simulations remain between residues Glu106 and Asp115, those residues in KirBac1.1 equivalent to Glu71 and Asp80 in KcsA. In the case of the open-state model, one molecule arrives to this site after 1 ns, a second one after two and a half ns, the third one after 12 ns, and the fourth one at 16 ns. Only the third one is replaced by a different water molecule, after 2 ns. This suggests that these buried water molecules behave as a component of the filter; they do not tend to exchange with bulk water or water molecules within the filter and their motion is strongly coupled with those of the surrounding protein. Furthermore, their dynamics does not seem to be controlled by the global conformation of the protein.

Below the selectivity filter, the channel opens in a wide cavity lined by hydrophobic residues. The volume of this central cavity is smaller in KirBac1.1 than in KcsA; only 20 water molecules were reported in the crystal structure of the closed channel versus 27 in the crystal structure of KcsA. Besides, in contrast to KcsA, one feature of the KirBac1.1 channel is that the pore helices no longer point directly to the center of the channel cavity and therefore the four pore helices are misaligned. Previously, it was observed experimentally that the negative stained crystals showed in the open conformation that the pore became hydrophilic, and it was filled with highly hydrophilic stain,[13] which correlates with the observations described from the MD simulations.

In the present simulations, we observed that the total number of water molecules in the closed channel, those reported in PDB 1P7B plus some others which were added (see methods), remain in the cavity during the 20 ns period. The number is nearly constant and equal to about 31. Initially, the same number of water molecules was added to the cavity of the open-state model and it was later observed that as time evolved, water entered the channel until the volume of the chamber was filled. The distance between the intracellular side of the selectivity filter and the lower end of the channel is about 70 Å, with the bulk of the IC domain lying about 40 Å below the lipid bilayer. At the cytosolic end of the transmembrane region, there are hydrophobic residues in each subunit which form a girdle narrow enough to exclude water from entering the pore. Therefore, water makes its way along the pore axis, perpendicular to the bilayer. At around 12 ns, a plateau of ca. 90 water molecules is reached inside the open-state channel. Water inside the open pore is rather dynamic, and most of the water molecules migrating in or out of the cavity have transit residence times varying between 0.2 and 0.4 ns.

In simulations of the open-state model, the total dipole of the cavity waters varies from 19 to 199 D, with an average total dipole, calculated at the center of mass of the TM domain of the protein, of 47 D. This contrasts with the equivalent value for the simulations of the closed-state model of 35 D. In both the closed- and open-state models, the average dipole moment of the *x* and *y* components is similar in magnitude and direction while the average magnitude of the *z* component is double their value, though larger fluctuations are observed. Interestingly, the direction of the total dipole in the open model is opposite to that of the closed model. The contribution of the pore helix dipole is similar in both of them, but in the case of the open-state model, the M2 helices also have an effect which is different from zero. This could explain why the average dipole of the water in the cavity has a different sign.

During the first nanosecond of the simulation of the open-state model, when a K^+ ion enters the cavity from the intracellular side heading toward the selectivity filter, the average dipole contribution of the water molecules vanishes. This is to be expected, due to the self-arrangement of the water molecules in a symmetric manner around the ion.

Dynamics of K^+ Permeation through the Open- and Closed-State Models. Movements of K^+ ions and water molecules were examined in terms of their position along the pore axis, which corresponds to the principal symmetry axis of the protein. In the crystal structure of KirBac1.1, only three binding sites were described within the selectivity filter:[4] S1, S2, and S3. An extracellular binding site was also observed, S0. Two other higher resolution structures of a different inwardly rectifying K^+ channel, KirBac3.1, at 2.6 and 2.85 Å, have also been deposited in the protein data bank (PDBs 1XL6 and 1XL4). In all cases, the configuration of ions and water molecules in the selectivity filter is described as an averaged view of alternate configurations. Certainly, various configurations of ions and water molecules in the selectivity filter could be proposed from this crystallographic data.

In the simulations reported here, ions were initially placed at sites S0, S1, and S3 and water molecules at sites S2 and S4, in both the closed- and open-state models. No ions were placed in the cavity. Figure 2 shows the trajectory of the ions along the pore axis during the length of the simulation. The behavior of the selectivity filter and the ions in the closed model appears

(27) Zhou, Y.; Morais-Cabral, J. H.; Kaufman, A.; MacKinnon, R. *Nature* **2001**, *414*, 43−48.

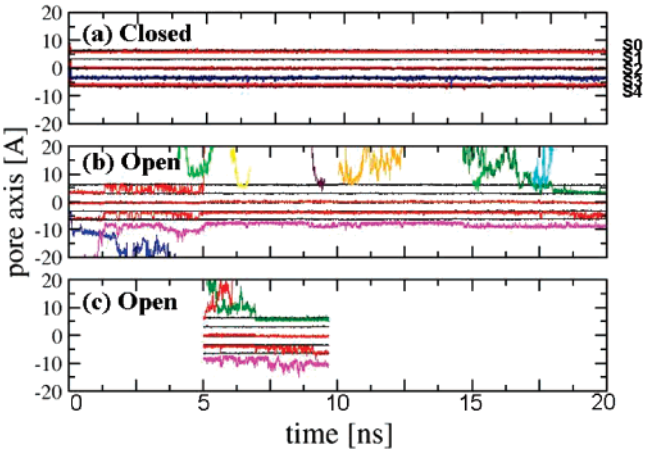

Figure 2. Trajectories of K^+ ions and water molecules along the pore axis of (a) the closed-state model and (b and c) the open-state model of KirBac1.1. In the three plots, the black horizontal lines correspond to the binding sites of the selectivity filter, labeled S0 to S4. (a) Trajectories of K^+ ions (in red) and water molecules (in blue) along the symmetry axis of the closed model of KirBac1.1. Ions were initially placed in S0, S1, and S3. Those in S1 and S3 quickly traveled to S2 and S4. (b) The same initial arrangement of ions and water was established in the simulation of the open model. However, the behavior of the ions is different, and various transitions inside the selectivity filter are observed. The trajectory of a K^+ ion that enters the channel from the intracellular side is colored in magenta. Positions of ions that approach S0 from the extracellular side are also represented in various colors (cyan, light green, green, yellow, orange, and dark purple). (c) To establish the sensitivity of the results to the ion parameters, the default ion parameters in the CHARMM force field were also used. Trajectories along the pore axis of the ions which were initially inside the selectivity are represented in red; in magenta is the ion that enters the protein through the IC domain and in green is an ion that approaches the protein from the extracellular solution.

to be indistinguishable from that of previous simulations which were based on the closed state of KirBac1.1 or the KcsA channel.[9,28,29] The positions of the K^+ ions in the filter remained more or less fixed relative to the carbonyl oxygens of the TVGYG motif. Initially, during the first few picoseconds, the ion in S0 travels toward the bulk, but it quickly returns to its original site. In contrast, ions in the selectivity filter jumped very quickly, during the first nanosecond, from S1 and S3 to S2 and S4 (Figure 2). During the 20 ns simulation, ions remain in the [S0, S2, S4] state, which has already been reported in simulations of this channel[30] and the KcsA channel. Free-energy perturbation and umbrella sampling calculations have suggested the [S0, S2, S4] configuration as the most stable configuration of ions in other K^+ channels.[8,31]

In contrast, configurations of ions in the selectivity filter of the closed model similar to those reported in ref 32, [S1, S4] or [S3, S4], are not observed in the present study. There are many differences between the set-ups of these simulations and those in ref 32, such as the number of water molecules in the cavity, minor differences in the protonation states of the channel transmembranes, the force fields employed for protein, water, and particularly for ions, etc. We are inclined to say that the main differences between the results presented here and those in ref 32 might be due to the parameters used for the ions. We agree with Hellgren et al.[32] that many more extensive simulations would be necessary to fully characterize all the possible configurations of ions in the selectivity filter of this family of K^+ channels during permeation.

A more complex scenario was observed in the simulation of the open-state model (Figure 2). In the first few picoseconds, ions move from [S0, S1, S3] to [S1, S2, S4], and this state remains for the first 2 ns of the simulation. During that time, S3 is empty, as the water molecule in that site escapes after about 100 ps to the "cavity" of the channel. In the meantime, a K^+ ion from the intracellular side makes its way through the open pore until it reaches the lower side of the selectivity filter in over 1 ns of dynamics. Afterward, for over 3 ns, there is a concerted motion upward−downward of the four ions interchanging sites on a picosecond time scale. They move from [S0, S2, S3, S4*] to [S1, S2, S4, S4_ext]. S4_ext is defined as a site below the selectivity filter. In general, the S4 site is never occupied by an ion; instead, there is a water molecule displacing the K^+ ion from the geometrical center of site S4; this situation is denoted by S4* to distinguish it from S4 where the ion sits perfectly between the eight carbonyl oxygens of the Thr110 amino acids.

Originally, when the ion first enters the filter from the IC domain, it goes straight to the center of S4 where there is another K^+ ion, which is displaced to an empty S3 site. The ion at S2 stays, and the ion at S1 moves to an intermediate position between S1 and S0. Then, the ion in S4 moves to one side of S4, leaving space for a water molecule to enter between this K and the one at S3. From this moment on, S4 seems always occupied by a water molecule and a K^+ ion; the ion lies slightly out of the geometric center of this site, and there is always a water molecule between this ion and the one at S3. Figure 3 shows three different views of a snapshot of the simulation of the open-state model where it can be observed that the ion at S4 (in orange) is not completely aligned with the ions in S2 and S3 (in green). It can also be observed that S1 can accommodate either one or two water molecules at a time.

Once the K^+ ion at S4 is off center, an ion occupies the center of S0 (in purple), and there are concerted movements of all the ions jumping up and down. At 5 ns, the ion at S0 leaves and the configuration [S2, S3, S4*] seems to be the preferred one for the remaining 11 ns. During this time, we observed that several ions from the bulk solution approach S0 in three different occasions for periods of 500 ps up to 1 ns. Ions at S2 and S3 remain in their positions, but the position of the ion at S4 is affected, and it is usually displaced an extra 1 or 2 Å from the ion in S3. After 15 ns, the ion in S4 travels about 5 Å toward the intracellular side of the pore. At this point, the selectivity filter is occupied by water molecules and a K^+ ion at S2 and S3. At 17 ns, a couple of K^+ ions approach the channel from the extracellular side and one of them manages its way to S0 where it remains for over 1 ns. Then it moves to S1, and it remains there for the last 2 ns of the simulation. While this takes place, the K^+ at S3 also starts moving toward S4. The final situation is one where three ions are inside the selectivity filter, at S1, S2, and S3, and the fourth ion is at S4 but slightly displaced from its geometrical center by a water molecule.

In general, only flipping of the carbonyl atoms of Gly114 (top residue of the selectivity filter facing the bulk solution) is observed. It can also be noted that the ion at S2 is always well

(28) Berneche, S.; Roux, B. *Biophys. J.* **2000**, *78*, 2900−2917.
(29) Luzhkov, V. B.; Aqvist, J. *Biochim. Biophys. Acta* **2001**, *1548*, 194−202.
(30) Domene, C.; Grottesi, A.; Sansom, M. S. P. *Biophys. J.* **2004**, *87*, 256−267.
(31) Aqvist, J.; Luzhkov, V. *Nature* **2000**, *404*, 881−884.
(32) Hellgren, M.; Sandberg, L.; Edholm, O. *Biophys. Chem.* **2006**, *120*, 1−9.

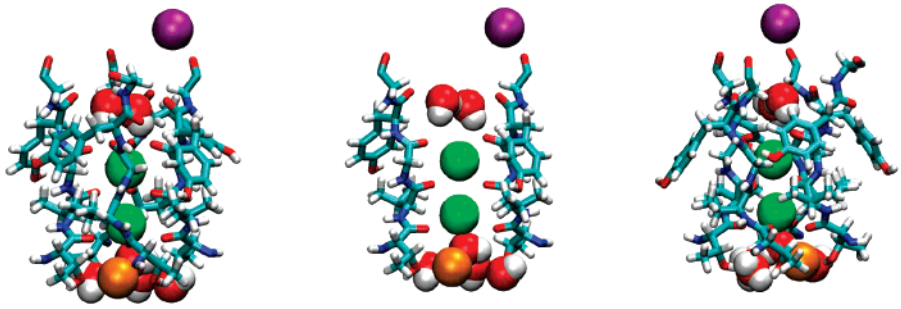

Figure 3. Dynamics of water and ions in the selectivity filter of the open-state model of the KirBac1.1 channel. The figure shows three different views from a snapshot of the simulation of the open model where it can be observed that the ion in S4 (in orange) is not completely aligned with the ions in S2 and S3 (in green). In the central representation, only two out of the four chains are shown for simplicity. The four chains are shown in the right and left representations.

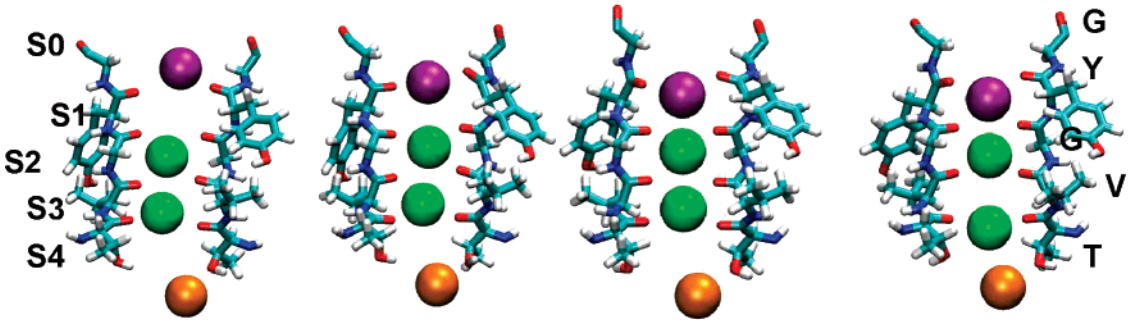

Figure 4. Snapshots of the selectivity filter in the open model of KirBac1.1. The TVGYG motif is shown in licorice representation for two of the four subunits. The K^+ ion entering the filter from the extracellular side is represented with a purple sphere, those inside the selectivity filter since the beginning of the simulation are represented in green, and the K^+ ion which enters the channel from the intracellular side is represented by an orange sphere. For simplicity, water molecules are not represented.

packed by the surrounding carbonyl oxygen atoms. S1 and S3 are implicated in a sort of "breathing" motion as the ions move up and down. This situation where the sites tend to '"swell" or "shrink" depending on their occupancy was first described by Luzhkov et al.,[29] though in that occasion it referred to the situation when the filter was occupied by water and ions alternating. Then, the sites with water swelled while those sites accommodating ions tended to shrink. Significant reorientations are almost absent apart from those involving Gly114, especially when the selectivity filter is highly occupied by ions.

In principle, this single trajectory suggests that the organization of ions in the selectivity filter of a channel in an open conformation is different from that in the closed conformation. One configuration which seems to be favorable is one where two ions occupy consecutive positions, either S1 and S2 or S2 and S3 (Figure 4). A configuration with the filter occupied by three ions also seems to be possible. In general, when the filter is occupied by three ions at a time, and one of them occupies S4, this ion is not totally aligned along the *z* axis with the other two ions.

Recently, similar events have been described in simulations of an open-state K^+ channel, Kv1.2.[33] Certainly, these events ought to be characterized using more sophisticated calculations in order to be able to energetically rank the configurations described above. These results might be relevant in the context of the many simulation studies that have addressed issues of ion permeation and selectivity based on the closed-state structure of KcsA. An underlying assumption of previous simulations is that the conformational behavior of the filter region is not significantly altered by the opening of the cytoplasmic gate, which also seems to be valid in our simulations. However, other factors should be affecting the dynamics of the ions in the selectivity filter and its occupancy, as it appears that the behavior of the ions in the open-state model is different from those in the closed model. One contributing factor might come from the water in the cavity, whose average dipole has the opposite contribution in each case, as shown before.

Energetics of Ion Permeation and Ion Flows. For any charged species there is a purely electrostatic dielectric barrier to move from a high-dielectric medium to a low-dielectric medium, generally referred to as the Born energy. Clearly, the barriers that an ion has to overcome to cross the channel pore in the closed- and open-state models are very different. The internal profile of the channel during the simulations was computed with the *HOLE* program, in both the closed- and open-state models (Figure 5). The size of the pore at the center of the lipid bilayer was 6 Å in the closed-state model and 11 Å in the open-state model. A larger difference between the internal radii in the two models was observed on the intracellular side of the pore, which acts as the channel gate. The internal radius falls below 2 Å (the permeant ion size) in the closed-state model, while in the open-state model the intracellular cavity is connected to the extracellular domain without any interruption.

As previously mentioned, it is not feasible to calculate meaningful ionic currents from MD simulations at present due to the limitations in the time scales of MD. Therefore, PB and

(33) Khalili-Araghi, F.; Tajkhorshid, E.; Schulten, K. *Biophys. J.* **2006**, *91*, L72−4.

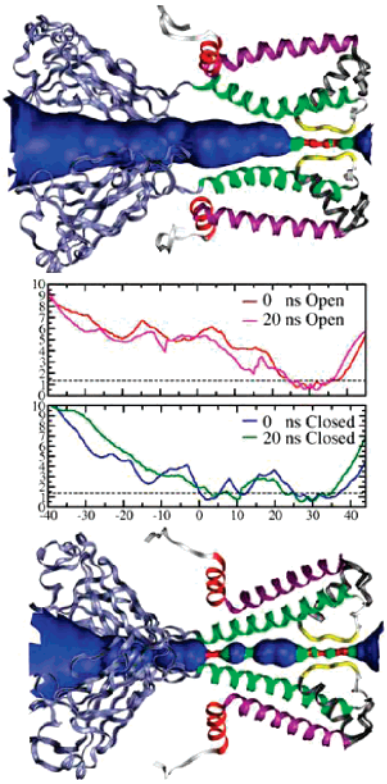

Figure 5. Pore profiles of the closed (bottom) and open models (top). Radius of the pore (Å) versus position along the channel axis (Å); top panel corresponds to the pore profile at 0 ns (red) and 20 ns (magenta) of the open model, and bottom panel corresponds to the pore profile at 0 ns (blue) and 20 ns (green) of the closed channel. The figures are the representation at 0 ns. Two monomers of the open (top) and closed (bottom) models are shown superimposed upon a representation of the diameter of the central ion conduction path. The red volume represents the place where there is not enough space for a water molecule to pass, the green volume is where one or two molecules could fit, and the blue volume corresponds to the space where more than two water molecules can fit.

PNP theories were used to investigate the energetics of ion translocation through the model channels and ionic fluxes.

A membrane potential of −100 mV was used in the PNP calculations, both for the open- and the closed-channel models. This membrane potential is physiologically relevant for the inward rectifier channel, such as KirBac1.1. The physiological function of these channels is to increase the membrane permeability to potassium ions at negative membrane potentials. Therefore, the probability of the open state is higher at negative membrane potentials. The higher open-state probability does not mean that inward rectifier channels are steadily open. Ion channels always flip between the open and the closed state, which justifies the comparison between the open and the closed model at the same membrane potential. The transmembrane potential was set to zero in the PB calculations. PB equations describe a steady state, with no ion fluxes. Therefore, it is not possible to study a nonequilibrium situation by the PB theory. Thus, PB and PNP theories were used to compare the open and the closed model in two different situations: with and without ion fluxes.

By application of the PB theory, the energetics of an ion moving through the channel in the closed- and open-state models was calculated. PB theory has been used before to show that a fully hydrated monovalent cation is stabilized at the center of

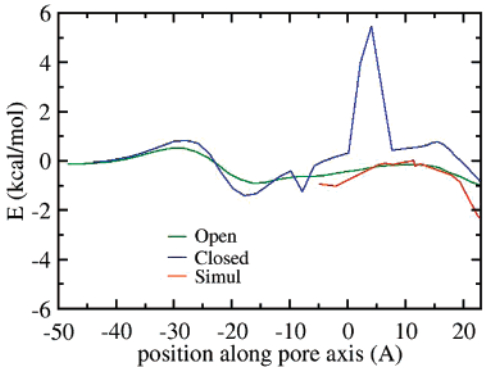

Figure 6. Energy profile of an ion transferred from the bulk into the channel (in kcal/mol) versus the position of the permeating ion along the channel pore. Values are for the open and closed models as well as for data obtained from calculations using snapshots of the simulation of the open channel where an ion travels from the IC domain up to the selectivity filter.

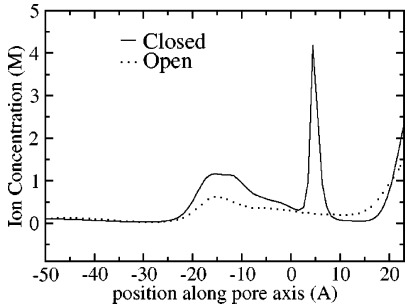

Figure 7. K^+ concentration along the channel axis using a boundary ion concentration of 100 mM and a membrane potential of 100 mV. The dotted line corresponds to the open model, and the continuous line corresponds to the closed model.

the KcsA cavity[34] by electrostatic interaction, and more recently, it has been used to investigate how the stability of an ion in the intracellular cavity is affected as the channel gate opens and the cavity becomes larger and contiguous to the intracellular solution.[35] Here, a similar analysis has been carried out to compare the characteristics of the closed- and open-state models of KirBac1.1. The electrostatic energy has been obtained for the process of moving an ion along the channel's pore, from the IC domain to the bottom of the selectivity filter (Figure 6). As expected, the radius of the channel pore has a dramatic effect on the energetic penalty for moving an ion from the bulk, high-dielectric region to the anisotropic dielectric environment of the channel pore. As the pore becomes larger, the intracellular cavity of the channel becomes an extended medium of the high-dielectric intracellular solution, and the energy barrier at the intracellular entrance of the cavity vanishes. In the open-state model, the cavity is at the same membrane potential as the internal solution. An open K^+ channel effectively thins the membrane for diffusing K^+ ions to approximately the 12 Å length of the selectivity filter. The access resistance for a K^+ ion diffusing between the cytoplasm and the selectivity filter is consequently low, which contributes to the high conductance of potassium channels.

Neither MD simulations of the length presented here nor PB theory are able to provide information about the ion fluxes through the protein. Therefore, to further characterize the movement of ions from the bulk solution to the intracellular

(34) Roux, B.; MacKinnon, R. *Science* **1999**, *285*, 100−102.
(35) Jogini, V.; Roux, B. *J. Mol. Biol.* **2005**, *354*, 272−288.

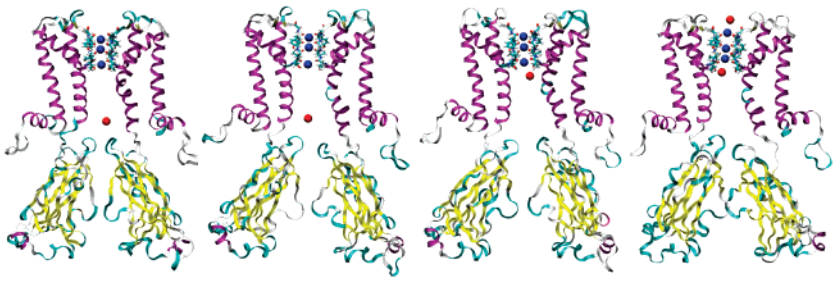

Figure 8. Some snapshots from the trajectory of the open model where a K^+ ion (red sphere) makes its way from the bulk solution to the central water cavity up to the selectivity filter. For simplicity, only two of the chains are represented.

cavity, the PNP electrodiffusion theory has also been employed. The concentration of K^+ along the channel axis exhibits strong differences between the closed- and open-state models (Figure 7). The main difference is located at the intracellular entrance of the channel ($z \sim 5$ Å), where the closed structure shows a sharp peak of K^+ concentration. This concentration peak overlaps with the energetic barrier shown in Figure 6. The simultaneous occurrence of an energetic barrier and a concentration peak, which seems inconsistent, is actually an artifact of the continuum approach, caused by the narrow cross section at the intracellular gate. To compute the energy profile of Figure 6, the product of the electrostatic potential and the electrical charge is summed over all the grid points. Then this value is compared to the equivalent value for a potassium ion in bulk. At the intracellular gate the channel is almost close (internal radius below 2 Å), and the K^+ ion partially overlaps with the protein, which causes the high energetic barrier. In contrast, Figure 7 shows the K^+ concentration in the grid elements along the channel axis, where there is no overlap between the ions and the protein atoms. The peak in concentration is caused by the narrow cross section of the channel in the closed-state model in the intracellular entrance corresponding to the aromatic rings of amino acids Phe114 of each monomer. The channel is occluded, and consequently, the ion current estimated by the PNP theory is close to zero; the closed model is physically shut at the intracellular gate (internal radius narrower than that of a K^+ ion), and continuum calculations just reveal this fact. In the open-state model, PNP calculations revealed an almost flat concentration profile, moving from the intracellular compartment to the bottom of the selectivity filter. The flat concentration profile agrees with the flat energy profile revealed by PB calculations. A slight increase in the K^+ concentration is located in the IC domain of the channel (-25 Å $< z < -5$ Å); the negatively charged amino acids of the intracellular domain account for this increase. No peak of K^+ concentration was revealed in the intracellular cavity (8 Å $< z <$ 18 Å). This data supports the experimental results obtained from functional mutations where it was demonstrated that K^+ channel function was remarkably unperturbed when positive charge changes occur near the permeant ions, at a location that should counteract pore helix electrostatic effects.[36] Therefore, it appears that pore helices in inward rectifier channels play a minor role in K^+ permeation. The main results are not affected by the specific snapshot chosen from the MD trajectory of the open-state model.

Macroscopic continuum electrostatic models, in which the solvent is described as a structureless dielectric medium, are particularly useful for revealing the dominant energetic factors related to ion permeation, as they provide a semiquantitative measure of the energetics of a K^+ ion as it is moved through the channels. However, they do not reveal the specific role of individual water molecules in confined regions, and it has been shown that an electrostatic continuum approach alone does not capture the essentials of ion permeation through pores in a low dielectric medium. Continuum theory uses a fixed atomic channel structure as an input, and ion-channel interactions depend dramatically on even the tiniest atomic flexibility of the channel. In the case of wide pores, this is not such a bad approximation, but in the case of narrow pores such as KirBac1.1, a more detailed atomistic approach is required that incorporates both the interaction of the water molecules with the ion and the protein flexibility. Here, advantage was taken of the fact that in the MD simulation one K^+ ion entered the open-state model from the intracellular side, providing a complete sequence of frames where the ion-channel interactions would be fully described (Figure 8). A set of calculations were carried out using snapshots from the MD trajectory of the open-state model. The energetics of ion translocation using this MD trajectory does not differ from those obtained when the ion was arbitrarily moved along the channel axis (Figure 6). The relatively small energy barriers for ion translocation in this region obtained from both the continuum electrostatics model and the spontaneous ion movement in the MD simulations indicate that ion−protein interactions largely compensate for ion−solvent interactions lost in the channel lumen. Ion channels provide an important challenge for continuum calculations because of the extreme sensitivity of ion permeation kinetics to the structural details of the pore. For this reason, in the present work we limited the discussion of the continuum model to the region below the selectivity filter which connects to the bulk solution at the intracellular side. The radius of the pore in the intracellular cavity of the open-state model is greater than 10 Å, which is reasonable to treat with a continuum solvent approach.

Conclusions

The availability of both closed- and open-state models for the KirBac1.1 K^+ channel has made possible the comparative analysis of permeation events of the same channel in two different conformations. To date, comparison between the open and closed states had only been made between families, but not within one family: for instance, KcsA[37] and KirBac1.1[4]

(36) Chatelain, F. C.; Alagem, N.; Xu, Q.; Pancaroglu, R.; Reuveny, E.; Minor, D. L., Jr. *Neuron* **2005**, *47*, 833−43.

(37) Doyle, D. A.; Cabral, J. M.; Pfuetzner, R. A.; Kuo, A. L.; Gulbis, J. M.; Cohen, S. L.; Chait, B. T.; MacKinnon, R. *Science* **1998**, *280*, 69−77.

for the closed state and MthK for the open state.[38] From the present studies, it can be concluded that the unfavorable barrier at the bundle crossing in the closed-state model disappears in the open-state model and ions are free to make their way through the protein. Analysis of the dynamics of the ions through these two models strongly suggests that the occupation of the selectivity filter depends upon the global conformation of the channel. As previously described by many studies of this and other K^+ channels, when the channel is closed the ion conduction involves transitions between two main sites, with two ions occupying the selectivity filter and separated by a water molecule. In contrast, in our open-state model, three to four ions move in a concerted motion during the conduction process which suggests the existence of a different conduction mechanism when the channel is in its open conformation. The selectivity filter, though maintaining a certain degree of flexibility to cope with these cooperative events, appears to be more "symmetrical" and robust in the simulations of the open-state model when it is occupied by an average of three ions. In KirBac1.1, sites S1 and S4 appear to be different from those in KcsA, as they can be occupied by more than one water molecule at a time. Further investigations will be required to clarify the precise chemical mechanism and energetics of permeation in this inward rectifier channel.

Acknowledgment. C.D. thanks The Royal Society for a University Research Fellowship, EPSRC (E004539), and the EPSRC National Service for Computational Chemistry Software. S.V. and M.L.K. thank the NIH and the NCSA Supercomputing facilities.

Supporting Information Available: Complete ref 18. This material is available free of charge via the Internet at http://pubs.acs.org.

JA075164V

(38) Jiang, Y. X.; Lee, A.; Chen, J. Y.; Cadene, M.; Chait, B. T.; MacKinnon, R. *Nature* **2002**, *417*, 523−526.